Polarons and bipolarons in *cis*-polyacetylene

Wolfram Utz and Wolfgang Förner*
Chair for Theoretical Chemistry, Friedrich-Alexander University, Egerlandstrasse 3, D-91058 Erlangen, Germany
(Received 10 February 1997; revised manuscript received 9 September 1997)

We present a parametrization for the Pariser-Parr-Pople Hamiltonian for the description of *cis*-polyacetylene (*c*PA). In contrast to *trans*-polyacetylene, we have to include symmetry breaking between neighboring sites into the Su-Schrieffer-Heeger-type one-electron part of the Hamiltonian. Our parametrization is based on correlated *ab initio* calculations on *cis*-hexatriene and on the results of independent calculations found in the literature. For open-shell systems (singly charged polarons) we use the annihilated unrestricted Hartree-Fock method to avoid the artificial spin contaminations inherent in UHF (unrestricted HF) calculations, which lead to the inclusion of fractions of the correlation energy in UHF total energies which cannot be controlled and are different for different systems and even for different geometries of the same system. Thus UHF is useless for the calculation of potential hypersurfaces and thus in turn for dynamical simulations. We find that in *c*PA singly-charged polarons are formed, while in doubly-charged chains stable bipolarons are found, although of a quite large width. This is in contrast to recent results reported by Shimoi and Abe [Y. Shimoi and S. Abe, Synth. Met. **69**, 687 (1995) and Phys. Rev. B **50**, 14 781 (1994)] who found that two singly-charged polarons are more stable for realistic parameter values than a doubly-charged bipolaron. We further find that the charged polarons are mobile in the chain and thus we conclude that polarons and bipolarons can serve as charge carriers (the latter ones spinless) in doped *c*PA. [S0163-1829(98)06706-X]

I. INTRODUCTION

The π-conjugated polymer polyacetylene[1] (PA) consists of weakly coupled linear chains of CH units. If the bonds would be of equal length, PA would be a quasi-one-dimensional metal, where the $2p_\pi$ orbitals of carbon form a half-filled π band. However, such states are not stable due to the Peierls distortion:[2] the system becomes more stable by the formation of alternating long and short CC bonds. The presence of sp^2 hybridized carbons allows the formation of two isomers, *c*PA and *t*PA where *t*PA is the thermodynamically stable one, while *c*PA is a metastable isomer, formed initially in the synthesis (see Ref. 2). The structures of the two isomers are sketched in Fig. 1.

It was found very early that *t*PA can be easily doped, both chemically and electrochemically, and becomes conducting upon doping with spinless charge transport at low doping levels. Further, *t*PA is photoconducting. The conductivity can be varied in a range of several orders of magnitude, at high doping levels to higher values than that of copper (see, e.g., Refs. 1, 2).

Naturally this behavior leads to a large number of theoretical investigations. At the beginning of these studies was the pioneering work of Su, Schrieffer, and Heeger[3,4] (SSH) who introduced the SSH Hamiltonian (corresponding in the continuum limit to well-known models in field theory[5]). The SSH model is basically of the Hückel type and electron-phonon interactions are included via an expansion of the next-neighbor resonance integrals in the bond lengths (projected onto the chain axis) up to the linear term (due to the small displacements of the CH units). Su, Schrieffer, and Heeger[3,4] found the existence of mobile domain walls between chain segments of different (but energetically degenerate) bond alternation phases *A* and *B*, i.e., solitons. These solitons are associated with an energy-level at midgap in the SSH model. The structures of the different phases and an idealized sketch of the soliton structure are shown in Fig. 2 where the u_i are the displacement coordinates of the CH unit i parallel to the chain axis.

Here neutral solitons carry one spin and thus their charged counterparts are spinless and mobile. If a chain without any deformation or unpaired electron is doped just with one electron, another nonlinear quasiparticle, namely a polaron, is formed. In the polaron case, a conformation *A*-*B*-*A* for the bond alternation phase is present and two levels (the lower one doubly, the upper one singly occupied in the negatively charged case) in the gap appear.[3,4] A further electron would enter the upper polaron level to form a doubly-charged bipolaron. However, in *t*PA the bipolarons cannot be stable, because the repulsion of the two charges separates them, without cost of energy because the phases *A* and *B* are degenerate. Thus instead of a bipolaron an unbound pair of charged solitons is formed.

However, it was established by electron nuclear double-resonance measurements that in *t*PA chains containing a neutral soliton a spin-density wave exists with alternating signs of the spin density on neighboring CH units, which cannot be explained by the simple SSH model.[6–10] Also ^{13}C-NMR (nuclear magnetic resonance) line shapes could not be explained by the SSH model.[11] Thus electron-electron interactions were introduced into the model with the help of on-site and nearest-neighbor Hubbard terms.[12,13] As a more reliable model the Pariser-Parr-Pople (PPP) Hamiltonian was

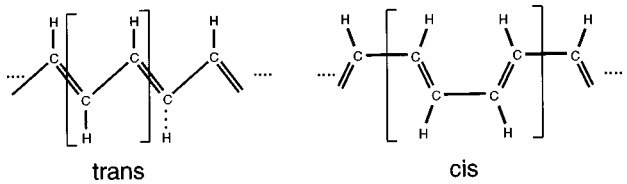

FIG. 1. Schematic sketch of the structures of *t*PA and *c*PA.

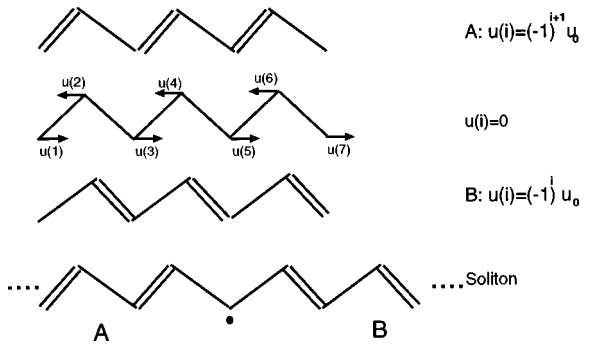

FIG. 2. Sketch of the structures of the different bond alternation phases A and B together with that of the metallic structure ($u_i = 0$) and of the soliton in tPA. u_0 is the dimerization constant, with an experimental value of 0.026 Å (Refs. 50 and 51).

used[14–16] and also other semiempirical and *ab initio* methods were applied.[17,18] In the case of the PPP model, it turned out that a reparametrization is necessary, because the SSH parameters contain already implicitly effects of electron-electron interactions and therefore are not consistent with the PPP model, which contains these effects explicitly.[19] However, in open shell cases the usually applied unrestricted Hartree-Fock method (UHF) could not be used because it introduces spin contaminations into the wave functions. This means, that the UHF state is not an eigenstate of the squared spin operator, which leads to even qualitatively wrong results, like the artificial preference of UHF for equidistant structures, which results in far too large and even diverging (with increasing chain length) soliton widths. Thus, instead of UHF one could use the annihilated UHF (AUHF) method which yields correct expectation values of the squared spin operator.[20] More recently, Rossi and Schneider[18] could show on the example of tPA that the SSH model could describe ground-state properties rather well, while in the case of excitations (also soliton or polaron excitations) the electron-electron interaction is important. Similar to Förner,[19,21] they conclude that a careful reparametrization of the PPP Hamiltonian is necessary.

However, there are not many conducting polymers known which exhibit a degenerate ground state like tPA (or pernigraniline) and thus allow soliton formation. The simplest such case is cPA where this degeneracy of the two minima is lifted. In this case we have again two different bond alternation phases, namely the so-called cis-transoid (A) and the trans-cisoid (B) structures, where experiments as well as theoretical studies indicate that the cis-transoid (A) phase is energetically favorable.[22–24] As in the case of tPA one can define a dimerization coordinate with one degree of freedom for each CH group (see the sketch in Fig. 3).

However, in contrast to tPA this coordinate in cPA is not parallel to the chain axis. As mentioned above, of the two PA isomers cPA is a metastable one and in the process of the PA synthesis one can obtain each desired ratio of the amount of tPA with that of cPA, where from a temperature of 180 °C no more cPA is found in the mixture.[1] Other conducting polymers without degenerate ground states are, e.g., polythiophene,[1] polyparaphenylene[25] or polypyrrole.[26] However, for our investigation we have chosen cPA because it is the simplest such case and therefore an ideal starting point for the investigation of this type of polymers.

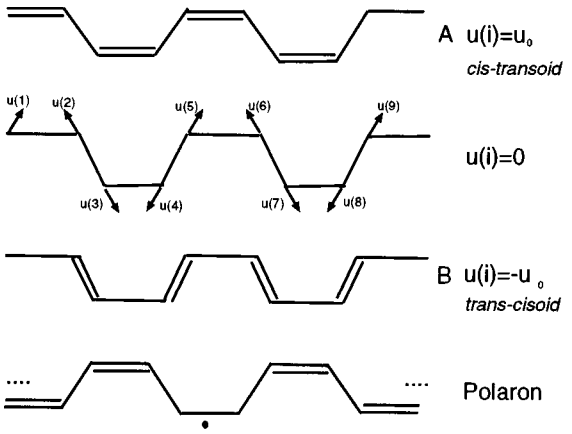

FIG. 3. Sketch of the structures of the different bond alternation phases A and B together with that of the metallic structure ($u_i = 0$) and of the polaron in cPA.

Theoretical investigations on cPA using SSH-type Hamiltonians go back to Brazowskii and Kirova,[27] Heeger[28] and Wang, Su, and Martino.[29] As discussed above, solitons turn out to be not a suitable excitation in these systems, because of the lifted degeneracy of the two phases, but two solitons become confined to form polarons or bipolarons, with a structure A-B-A in contrast to A-B for solitons, where in the central segment, the geometry of the B phase is not fully formed in the case of polarons. The length of the B phase is determined by a delicate balance between the energy gain from, e.g., charge separation and the energy loss due to formation of the energetically unfavorable B phase. Thus the possibility of polaron or bipolaron formation depends strongly on the individual structure of each material, and reparametrizations of model Hamiltonians are, in principle, necessary for each system separately, especially if the polymers contain groups other than CH.

In the literature some further previous investigations on cPA can be found. Shimoni and Abe published investigations using the PPP Hamiltonian in UHF approximation on exciton polarons[30] and on bipolarons[16,31] in cPA. However, the deficiencies of an UHF approach to open-shell systems were already mentioned above. cPA clusters of a size up to 40 CH units containing kink-antikink defects with the help of the local-density-functional approximation were studied by Ye *et al.*[13] Springborg[32] used an SSH-type Hamiltonian augmented with second-neighbor and on-site terms, while Suhai[24] investigated the stability of infinite chains of tPA and cPA with full translational symmetry on the *ab initio* HF level (in the case of tPA also with corrections due to electron correlation). Bredas and co-workers[22,33] performed similar studies with a different basis set. These studies yield important information about the degree of dimerization, the dimerization energy and the energy difference between the two phases, which are necessary for a parametrization of model Hamiltonians. Effects of Coulomb interactions between the electrons on the stability of bipolarons were investigated by Wen and Su.[34]

In this work we applied the PPP Hamiltonian to cPA using the AUHF approach. We present a scheme for a parametrization of this model (in this connection we discuss also shortly the problems connected with the UHF approximation) which can be used in a similar fashion also for other

conducting polymers. Further, we discuss dynamical simulations and geometry optimizations on singly and doubly charged *c*PA chains. The geometrical model we used for *c*PA is discussed in Appendix A.

II. METHOD

A. The PPP Hamiltonian in the AUHF approximation

The PPP model for the semiempirical description of the π electrons of a system (separated approximately from the rest of the electrons) is well known and described in detail in Refs. 35–39. The total energy of a system is thus given as a sum of different terms:

$$E^{\mathrm{tot}}=E^{\mathrm{pot}}+E^{\mathrm{kin}}=E^{\pi}+E^{nn}+E^{\sigma-\pi}+E^{\sigma}+E^{\mathrm{kin}}, \qquad (1)$$

where E^{π} denotes the energy of the π electrons, E^{nn} is the repulsion energy of the positively charged ionic cores, $E^{\sigma-\pi}$ is the interaction energy between σ and π electrons, E^{σ} is the σ-electron energy (a detailed description of this term is given in Appendix B), and E^{kin} is the kinetic energy of the ionic cores in case of time simulations (see below). In the PPP approximation $E^{\sigma-\pi}$ is formally assumed to vanish, thus $E^{\sigma-\pi}=0$ in our case. However, the term is included implicitely via the parametrization.

Using the mean-field (Hartree-Fock) approximation in UHF form, the wave function of the π electrons is written as a Slater determinant from different spatial orbitals for different spins. The orbital i for spin σ ($\sigma=\alpha$ or β) is written as a linear combination of basis functions, one at every site (orthogonalized linear combinations of a $2p_{\pi}$ function at each site):

$$\psi_i^{\sigma}(\underline{r})=\sum_{r}^{N} c_{ri}^{\sigma}\chi_r(\underline{r}), \qquad (2)$$

where r runs over all sites in a chain. Further we have the zero differential overlap approximation in the PPP model which states that

$$\chi_r^{*}(\underline{r})\chi_s(\underline{r})=|\chi_r(\underline{r})|^2\delta_{rs}. \qquad (3)$$

Note, that in our case the basis functions are assumed to be real. The integrals between the basis functions are the parameters entering the Hamiltonian. Performing the usual variational calculation, we obtain the coupled eigenvalue equations

$$\underline{\underline{F}}^{\sigma}\underline{c}_i^{\sigma}=\varepsilon_i^{\sigma}\underline{c}_i^{\sigma} \qquad (4)$$

for the unknown coefficient vectors $\underline{c}_i^{\sigma}$. The elements of the Fock matrices are given by ($\mu=\beta$ if $\sigma=\alpha$ and vice versa):

$$F_{rs}^{\sigma}=F_{rs}^{N}+\left[\gamma_{rr}P_{rr}^{\mu}+\sum_{t=1}^{N}(P_{tt}^{\alpha}+P_{tt}^{\beta})\gamma_{rt}(1-\delta_{rt})\right]\delta_{rs}$$
$$-P_{rs}^{\sigma}\gamma_{rs}(1-\delta_{rs}), \qquad (5)$$

where the one-electron part is

$$F_{rs}^{N}=\left[-I_r-\sum_{t=1}^{N} z_t\gamma_{rt}(1-\delta_{rt})\right]\delta_{rs}+\beta_{rs}. \qquad (6)$$

Here $I_r=11.54$ eV denotes the ionization potential of a CH unit,[40] $z_r=1$ is the charges of the ionic cores (CH^{+}) and $\gamma_{rr}=11.25$ eV is the on-site Hubbard repulsion.[19] This value stems from a previous parametrization of the PPP Hamiltonian[19] and is close to the usually quoted value of the difference between ionization potential and electron affinity of carbon (11.08 eV). The charge-density bond order matrices $\underline{\underline{P}}^{\sigma}$ (shortly called density matrices) are given by

$$P_{rs}^{\sigma}=\sum_{j=1}^{N} o_j^{\sigma}c_{rj}^{\sigma}c_{sj}^{\sigma}; \quad P_{rs}\equiv P_{rs}^{\alpha}+P_{rs}^{\beta}, \qquad (7)$$

where o_j^{σ} is the occupation number of the molecular orbital (MO) j for spin σ (0 or 1). Note, that we use real MO coefficients c_{rj}^{σ} in all our calculations.

For the two-electron integrals we use the Ohno approximation:[41]

$$\gamma_{rs}=a\left[\left(\frac{2a}{\gamma_{rr}+\gamma_{ss}}\right)^2+R_{rs}^2\right]^{-1/2}; \quad a=\frac{e^2}{4\pi\varepsilon_0}, \qquad (8)$$

where e is the elementary charge and ε_0 is the dielectric constant. The electron-phonon coupling matrix β is given as (note the symmetry breaking which leads to a lifting of the degeneracy of the phases A and B already on the SSH level):

$$\beta_{rs}=\beta(r)\delta_{s,r+1}(1-\delta_{rN})+\beta(r-1)\delta_{s,r-1}(1-\delta_{r1}),$$
$$\beta(r)=\begin{cases}-b_1-[u(r)-u(r+1)]a_1; & r \text{ even}\\ -b_2-[u(r)-u(r+1)]a_2; & r \text{ odd.}\end{cases} \qquad (9)$$

Here the parameters b_2 and a_2 describe the bonds parallel to the chain axis and b_1 and a_1 are the inclined ones. This form of the electron-phonon interaction was also used by Wang and Martino[12] in the framework of the SSH model of *c*PA.

The eigenvalue problem is solved by a self-consistent iteration, i.e., we need a guess for the density matrices $\underline{\underline{P}}^{\sigma}$. As guess for smaller chains (up to $N=10$) we use the results of a simple Hückel calculation, while for larger chains we use as guess the converged density matrices of shorter ones. Since we need accurate numerical gradients in the parametrization, we have to use a convergency threshold for the energy of 10^{-13} eV. This high accuracy leads especially for long chains to the necessity of a large number of iteration cycles (up to several thousands without using extrapolation techniques). The total π-electron energy and the ionic repulsion energy are given by

$$E^{\pi}=\frac{1}{2}\sum_{rs}\sum_{\sigma}(F_{rs}^{\sigma}+F_{rs}^{N})P_{rs}^{\sigma},$$

$$E^{nn}=\frac{1}{2}\sum_{rs}(1-\delta_{rs})z_r z_s\gamma_{rs}. \qquad (10)$$

As mentioned above, the UHF model has the disadvantage that the total wave function is not an eigenfunction of the squared spin operator. Investigations on *t*PA have shown[42] that with the UHF approximation one obtains a soliton width which diverges with increasing chain length. Further due to the spin contaminations in the UHF wave functions one obtains total energies which contain (unknown) fractions of the correlation energy which decrease exponen-

tially with increasing dimerization amplitude. Thus a UHF potential surface is even qualitatively wrong and UHF predicts an equidistant ground state for *t*PA in contradiction to experiment.[21] The most straightforward method to overcome this problem is the extended HF (EHF) method,[43,44] where the spin contaminations are projected out of the ansatz wave function before the variation is performed. However, the resulting equations are quite complicated and thus the method seems not to be feasible for time simulations on larger chains. Another possibility would be the restricted open-shell HF (ROHF) method, where the same spatial orbitals for different spins are used as in the restricted HF (RHF) but the occupation numbers of the orbitals are allowed to be 0, 1 or 2 (0 and 2 in the RHF). Unfortunately, ROHF cannot describe the spin polarization and is thus inappropriate for our use.

Finally, because of the experiences with this method in the *t*PA case[15,24] we decided to use the annihilated UHF (AUHF) method[45] where—starting from a guess with correct $\langle \hat{S}^2 \rangle$—the contamination coming from the next higher multiplicity is projected out at every self-consistent field iteration. This procedure usually converges to a state with an approximately correct expectation value of the squared spin operator independent of the chain length or geometry (e.g., an expectation value of the squared spin operator of $0.7506\hbar^2$ instead of the correct value of $3/4\hbar^2$ for doublet states in *c*PA). In the case of $\langle S^2 \rangle = 0\hbar^2$, AUHF makes it possible to describe spin polarizations of the closed-shell system, i.e., it does not necessarily converge to the RHF solution. However, one has to keep in mind that AUHF—besides all of its advantages—dissociates in the same way as RHF. Thus, for instance, H_2 gives an incorrect dissociation behavior with AUHF. In our optimizations and time simulations, however, displacements are usually far below the dissociation regions for the bonds. The annihilation operator is (see also Ref. 20, and references therein)

$$\hat{A}_{s+1} = \frac{\hat{S}^2 - (s+1)(s+2)}{\langle \hat{S}^2 \rangle - (s+1)(s+2)}. \tag{11}$$

The annihilated density matrices can be computed by simple matrix multiplications by the matrices formed directly from the MO coefficients. From the UHF density matrices $\underline{\underline{P}}^{\sigma}$ the annihilated matrices $\underline{\underline{J}}^{\sigma}$ ($\sigma = \alpha$ or β) are obtained as

$$\begin{aligned} M^2 \underline{\underline{J}}^{\alpha} = {} & [A^2 - 2A\ \mathrm{Tr}(\underline{\underline{P}}^{\alpha}\underline{\underline{P}}^{\beta}) - N\ \mathrm{Tr}(\underline{\underline{P}}^{\alpha}\underline{\underline{P}}^{\beta}) + 3\ \mathrm{Tr}(\underline{\underline{P}}^{\alpha}\underline{\underline{P}}^{\beta}) + pq - q + 2\ \mathrm{Tr}^2(\underline{\underline{P}}^{\alpha}\underline{\underline{P}}^{\beta}) - 2\ \mathrm{Tr}(\underline{\underline{P}}^{\alpha}\underline{\underline{P}}^{\beta}\underline{\underline{P}}^{\alpha}\underline{\underline{P}}^{\beta})]\underline{\underline{P}}^{\alpha} \\ & - [p - \mathrm{Tr}(\underline{\underline{P}}^{\alpha}\underline{\underline{P}}^{\beta})]\underline{\underline{P}}^{\beta} + \underline{\underline{P}}^{\beta}\underline{\underline{P}}^{\alpha}\underline{\underline{P}}^{\beta} + [N - 4\ \mathrm{Tr}(\underline{\underline{P}}^{\alpha}\underline{\underline{P}}^{\beta}) - 3 + 2A]\underline{\underline{P}}^{\alpha}\underline{\underline{P}}^{\beta}\underline{\underline{P}}^{\alpha} + \underline{\underline{P}}^{\alpha}\underline{\underline{P}}^{\beta} + \underline{\underline{P}}^{\beta}\underline{\underline{P}}^{\alpha}[2\ \mathrm{Tr}(\underline{\underline{P}}^{\alpha}\underline{\underline{P}}^{\beta}) - p + 1 - A] \\ & - 2[\underline{\underline{P}}^{\alpha}\underline{\underline{P}}^{\beta}\underline{\underline{P}}^{\alpha}\underline{\underline{P}}^{\beta} + \underline{\underline{P}}^{\beta}\underline{\underline{P}}^{\alpha}\underline{\underline{P}}^{\beta}\underline{\underline{P}}^{\alpha}] + 4\underline{\underline{P}}^{\alpha}\underline{\underline{P}}^{\beta}\underline{\underline{P}}^{\alpha}\underline{\underline{P}}^{\beta}\underline{\underline{P}}^{\alpha}, \end{aligned} \tag{12}$$

$$M^2 = A^2 + pq + [2 - 2A - N + \mathrm{Tr}(\underline{\underline{P}}^{\alpha}\underline{\underline{P}}^{\beta})]\mathrm{Tr}(\underline{\underline{P}}^{\alpha}\underline{\underline{P}}^{\beta}) - 2\ \mathrm{Tr}(\underline{\underline{P}}^{\alpha}\underline{\underline{P}}^{\beta}\underline{\underline{P}}^{\alpha}\underline{\underline{P}}^{\beta}). \tag{13}$$

Here Tr( ) denotes the trace of the argument in brackets, p is the number of α-spin electrons, q is that of the β-spin electrons $A = q - 2(s+1)$, $s = (p-q)/2$ and N is the total number $(p+q)$ of electrons. With A chosen as given above, the largest contaminating state is annihilated. $\underline{\underline{J}}^{\beta}$ is obtained by an interchange of α with β and p with q in the above equations.

B. Kinetic energy, time simulation, and geometry optimization

The kinetic energy in a time simulation is given by

$$E^{\mathrm{kin}} = \frac{1}{2}\, m_{\mathrm{CH}} \sum_{i=1}^{N} [\dot{\underline{r}}(i)]^2, \tag{14}$$

where the dot denotes a time derivative. Insertion of the explicit equation for the position vector (Appendix A) yields

$$\begin{aligned} E^{\mathrm{kin}} = \frac{1}{2}\, m_{\mathrm{CH}} &= \sum_{i=1}^{N} \left\{ \frac{d}{dt} [\underline{r}_d(i) + u(i)g(i)] \right\}^2 \\ &= \frac{1}{2}\, m_{\mathrm{CH}} \sum_{i=1}^{N} [\dot{u}(i)g(i)]^2 = \frac{1}{2}\, m_{\mathrm{eff}} \sum_{i=1}^{N} [\dot{u}(i)]^2, \end{aligned}$$

$$m_{\mathrm{eff}} \equiv m_{\mathrm{CH}}[g(i)]^2, \tag{15}$$

where m_{CH} denotes the mass of a CH group. In the Born-Oppenheimer approximation we can consider the CH groups as classical particles moving in the potential E^{pot}. Thus Newton's equations of motion are

$$m_{\mathrm{eff}} \frac{d^2 u(i)}{dt^2} = -\frac{\partial E^{\mathrm{pot}}}{\partial u(i)} = F(i). \tag{16}$$

Explicit equations for the derivatives are detailed in Appendixes A and C. With the geometries $u(i,t_0)$ at any time t_0 and their time derivatives $v(i,t_0)$, we can compute in a simple one-step procedure the positions and velocities at the time $t_0 + \Delta t$ by

$$\begin{aligned} \nu(i, t_0 + \Delta t) &= \nu(i, t_0) + \frac{F(i, t_0)}{m_{\mathrm{eff}}}\, \Delta t, \\ u(i, t_0 + \Delta t) &= u(i, t_0) + \nu(i, t_0 + \Delta t)\Delta t. \end{aligned} \tag{17}$$

During a simulation, the conservation of total energy is checked to ensure that the time step Δt was chosen small enough. Geometry optimization can be performed by reducing all velocities after a time step with the same factor or by using a Fletcher-Powell algorithm using the energy gradients.

C. Parametrization

As the first step of our numerical work we had to perform a parametrization of the model based on the results of independent theoretical calculations and/or experiments. An orientation is the reparametrization of the PPP model for *t*PA performed previously.[19,21] Here $a=a_1=a_2=1.9$ eV/Å and $b=b_1=b_2=2.4$ eV were found, with the electron-phonon interaction a less than half of the SSH values. This had one main reason: A part of the electron-phonon interactions is included via the geometry dependence of the integrals in the γ's and not in the one-electron part. Thus in a PPP Hamiltonian electron-phonon and electron-electron interactions cannot be trivially separated from each other. And the differences in the energies of the two bond alternation phases are already contained in the γ's and therefore, $|a_1-a_2|$ could be much smaller than it was reported for pure SSH Hamiltonians or Hubbard models (where only the on-site term of the electron-electron interactions is present).[26,27] The same holds also for PPP Hamiltonians where the geometry dependence of the γ's is neglected, as in the work of Shimoi and Abe.[16,30,31] The results of these types of studies could be misleading, because the electron-phonon interactions contained only in the one-electron part of the model could have other effects than is the case in a more realistic model, where electron-phonon interactions are contained both in the one- and in the two-electron part of the Hamiltonian. Since this property of the interaction follows clearly and unambiguously from the geometry dependence of all integrals in an *ab initio* treatment of a system, we consider a PPP Hamiltonian with geometry dependent γ's (Ohno formula) as more realistic than geometry-independent two-electron interaction parameters.

As a first step we have to get an idea about the range of the one-electron parameters which can be considered as realistic. Note that the parameter value $a=1.9$ eV/Å found for *t*PA (Ref. 21) is related to the bond length projected on the polymer axis in *t*PA. In the case of our choice of the generalized coordinate u for *c*PA (see Appendix A), this corresponds to a value of 0.08 eV/Å. Thus the region for the parameters which can be considered as realistic and has to be investigated is

$$1.9 \text{ eV} \leqslant b_1, \quad b_2 \leqslant 3.6 \text{ eV},$$

$$0.05 \text{ eV/Å} \leqslant a_1, \quad a_2 \leqslant 0.13 \text{ eV/Å}. \tag{18}$$

The on-site two-electron term γ_{rr} is not considered as a variable because the symmetry breaking in *c*PA is already contained in the geometry dependence of the γ_{rs}, which all depend on the constant γ_{rr} and on the distance between sites r and s. In contrast to *t*PA we have for *c*PA the behavior

$$\gamma_{r,r+2}|_{u=u_0} \neq \gamma_{r,r+2}|_{u=-u_0}, \tag{19}$$

which is exactly the desired symmetry breaking. Note that a double-well potential (which is assumed for *c*PA in general, see *ab initio* results below) cannot exist for finite even-numbered chains, because in that case a negative value of u implies a structure with two unsaturated carbons at the chain ends. This is not the case in calculations on an infinite chain with periodic boundary conditions or for odd-numbered small chains because in the latter case both $u=u_0$ and $u=-u_0$ imply one unsaturated carbon at one of the chain ends. We consider periodic boundary conditions in finite chains as unrealistic and thus use open chain ends throughout.

First of all we have to consider a basic qualitative result of *ab initio* calculations on the infinite chain (see Refs. 29, 30, 32, and 33 and Table I) for our parametrization: there exists an absolute energy minimum for *c*PA at $u=u_0$ (A phase), accompanied by a local maximum around $u=0$ and a local minimum around $u=-u_0$ (B phase) where the length of CC double bonds and CC single bonds in both phases should not differ too much. Thus we need to have a set of parameters which yields a double-well potential with the A phase being lower in energy than the B phase. Further we have performed *ab initio* HF/MP2 calculations on M points $u(I)$ with $0<u(I)<3$ using a 6-31G** basis set on *cis*-hexatriene again using the GAUSSIAN94 program package. Since such calculations can be considered as very reliable for a potential surface in the A-phase region, we have to require that our PPP energies are as close as possible to this potential curve (which shows a minimum at $u=u_0$ and thus the minimum requirement is fulfilled automatically if this potential is reproduced). Again we want to include the correlation effects via the parameter values into a PPP/RHF calculation on *cis*-hexatriene. Thus we can reduce our four-dimensional parameter space with the help of the following three general requirements:

(1) We require that at $u=u_m$ (u_m close to 0, equidistant chain) the derivative of the sum of the total π-electron and nuclear repulsion energies with respect to u has to vanish for odd N. This implies

$$\left.\frac{d(E^{\pi}+E^{nn})}{du}\right|_{u=u_m}=0, \tag{20}$$

and thus yields the dependence of one of the parameters, in our case we have chosen a_1, as a function (numerically given) of the other three:

$$a_1=a_1(b_1,b_2,a_2). \tag{21}$$

(2) For $N=6$ and $0<u(I)<3$ where I counts the M calculated *ab inito* values of the potential, $E^{\mathrm{MP2}}[u(I)]$, we require that the deviations of our total PPP energy values, $E^{\mathrm{tot}}[u(I)]$, from $E^{\mathrm{MP2}}[u(I)]$ is minimal and vanishes ideally:

$$\Delta E=\sum_{I=1}^{M}\{E^{\mathrm{tot}}[u(I)]-E^{\mathrm{MP2}}[u(I)]\}=0. \tag{22}$$

This yields numerically a second parameter (we have chosen b_2) as a function of the other three, with one of them being dependent already by virtue of condition (1):

$$b_2=b_2(a_1,a_2,b_1)=b_2(a_2,b_1). \tag{23}$$

(3) At $u=-u_0$ we require that for odd N the derivative of the total PPP energy with respect to u vanishes:

$$\left.\frac{dE^{\mathrm{tot}}}{du}\right|_{u=-u_0}=0. \tag{24}$$

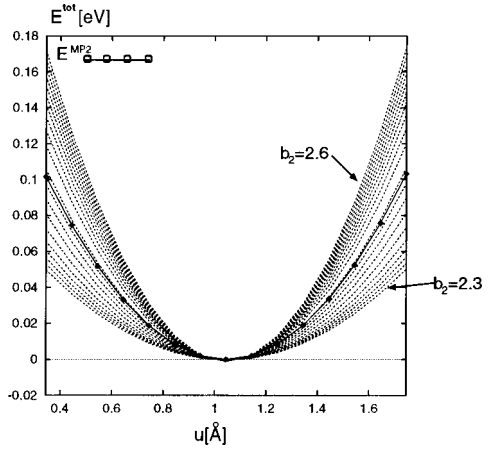

FIG. 4. E^{tot} (AUHF) as a function of the coordinate u for different values of b_2 and $b_1=2.4$ eV, $a_2=0.6$ eV/Å, $N=6$ (dashed lines) in comparison to E^{MP2} (solid lines).

This condition yields together with (1) and (2) a third parameter as a function (again numerically given) of the last free one:

$$a_2=a_2(a_1,b_1,b_2)=a_2(b_1). \tag{25}$$

In detail, the requirements yield the following:

(1) Numerically we found that the derivative of the total π-electron energy with respect to u at $u=u_m$ as a function of the parameter a_1 for any fixed parameter triple (a_2,b_1,b_2) is approximately linear. This yields a very simple procedure for the determination of a_1 for any triple of the other parameters: for two test values a_1^1 and a_1^2 we computed the above derivative at $u=u_m$. Then with the help of successive linear extra- and interpolations, a_1 is determined such that the absolute value of the derivative at $u=u_m$ is smaller as a prescribed threshold value chosen as 10^{-7} eV/Å. We use here the value of u_m which is the minimum of E^{σ} (see Appendix C) instead of $u=0$ since this choice significantly simplifies the numerical work and $u_m=0.0023$ Å is a very small deviation from the equidistant case. Further we found that for any pair (b_1,b_2) the function $a_1=a_1(a_2)$ is also linear.

(2) Figure 4 shows as an example the MP2 energies in comparison to the potential E^{tot} calculated for different values of b_2 for $b_1=2.4$ eV (AUHF case). We have chosen here the simple differences ΔE instead of their absolute values because in the former case we can obtain b_2 as a function of b_1 for any fixed pair (a_1,a_2) by a simple Hermite interpolation. We found that errors made by the use of ΔE instead of the absolute values are negligible. It turned out that $b_2=b_2(b_1,a_2)$ is a very simple function, in a very good first approximation, even linear.

(3) The zeroes of the derivative of E^{tot} with respect to u at $u=-u_0$ can again be determined by a simple Hermite interpolation. However, note that the accuracy of the derivative for $N>15$ can become quite low in the numerical differentiation.

We performed the parametrization procedure both for the UHF and the AUHF model. However, for the simplest SSH Hamiltonian our procedure is not applicable: In this case it is possible to fulfill conditions (1) and (2), but then it is not possible to meet condition (3). Crucial for this failure is condition (2): as in the tPA case[19,21] it is not possible to reproduce an MP2 potential with the SSH model and simultaneously fulfill the extrema conditions. In the AUHF case, we obtain a nearly linear dependence of b_2 on b_1. It is interesting to note that the free parameter b_1 is in a direct relation to the dimerization energy

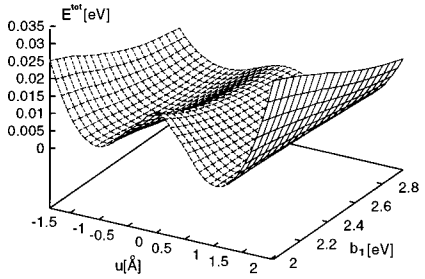

FIG. 5. E^{tot} (AUHF) as function of u and the remaining free parameter b_1 (the other three parameters are determined such that conditions 1 to 3 are fulfilled for $N=9$.

$$E^D=\frac{1}{N}\left(E^{\mathrm{tot}}\big|_{u=u_m}-E^{\mathrm{tot}}\big|_{u=u_0}\right) \tag{26}$$

and thus the choice of b_1 can be based on physical arguments. Further the parameter b_1 is also related to the symmetry breaking

$$E^{DD}=\frac{1}{N}\left(E^{\mathrm{tot}}\big|_{u=-u_0}-E^{\mathrm{tot}}\big|_{u=u_0}\right) \tag{27}$$

however, more weakly. If we change b_1 by 1 eV, then E^D changes by 8 meV and E^{DD} only by 1.8 meV. Increasing b_1 decreases E^D and E^{DD}. Further, shifting the left minimum from $-u_0$ to $-u_0+\Delta$ by a positive Δ increases E^{DD} and decreases E^D. In Fig. 5 we show the potential E^{tot} as function of u and the remaining free parameter b_1 for $N=9$ (AUHF case).

Here the dependence of the dimerization energy on the parameter b_1 can be clearly seen. This dependence can be used to take a value of b_1 where the E^D is correct according to calculations published previously. However, on the other hand, this fixes also E^{DD}, what might lead to problems.

It turned out that it is rather troublesome to perform the above-mentioned procedure for larger chains. Fortunately we found that in the AUHF case conditions 1–3 can be fulfilled for larger chains with the same set of parameters determined for $N=9$. Only the values of the spring constant K, the dimerization E^D, and the symmetry breaking E^{DD} then become a function of the chain length N, which converges for increasing N. A feature that is not present in the UHF case: Here one needs different sets of parameters for different chain lengths, which is quite an unphysical situation and has its reason in the spin contaminations which increase considerably with increasing N. Further, the UHF method tends to prefer the *trans-cisoid* phase more, the larger N becomes. This is again an indication of the unphysical nature of the UHF results due to spin contaminations. We show in Table I values for E^D and E^{DD} found in the literature.

TABLE I. Theoretical values for E^D and E^{DD} published previously in the literature (*ab initio* minimal basis calculations). E(ex) denotes values for *c*PA which are extrapolated from the directly calculated values on the basis of HF/MP4 calculations for *t*PA by Suhai (Ref. 47) ($E^D = 22.75$ meV/CH; all values in meV/CH).

E^D (*c*PA)	E^{DD} (*c*PA)	E^D (*t*PA)	Ref.	E^D(ex)	E^{DD}(ex)
206	54	182	24	25.7	6.7
75	5	155	48	11.0	0.7
140	5	190	49	16.7	0.7

Our values from the parametrized PPP model are slightly above the E^D values given in the table and between the values for E^{DD} which show a large difference anyway. Therefore these values can be used just as a qualitative orientation and not as definite physical quantities. More thorough *ab initio* calculations on *c*PA in a better basis set and with correlation corrections would be necessary. In our calculation we use five sets of parameters: Ia and Ib have the left minimum at $u = -u_0$, IIa, IIb, and IIc at $u = -u_0 + 0.1$. Group II was introduced to get also larger values for E^{DD} as indicated by the calculation by Shuhai.[24] The parameter sets together with the resulting symmetry breaking and dimerization energies are given in Table II.

III. GROUND-STATE OPTIMIZATIONS

We performed optimizations of *c*PA chains (even number of carbons) doped with one and two electrons, respectively. In our geometry optimizations we used a ''time step'' of 0.5 fs and a damping factor for the velocities in each time step of 0.3. Some calculations were additionally carried out using a Fletcher-Powell algorithm[46] to enhance convergency. The geometry was optimized until the changes in the coordinates $u(i)$ between two consecutive ''time steps'' were less than 10^{-4} Å. To determine the width of the (broad) bipolaron structures correctly, we performed geometry optimizations starting from the ground-state structure of the doped system as a first step and compared these results with optimizations carried out with starting geometries of a greater width than the one found in the first step. As the unit for the determination of distances we use δ, which is the length of a C═C—C unit in *cistrans*-conformation, projected onto the chain axis. This is half of the length of an elementary cell of *c*PA (2.19 Å) in our model. For the calculations we use the AUHF method and, for comparison, UHF.

In the case of a singly-charged chain, the result of the optimization is the formation of a singly-charged polaron in the center of the chains. Associated with this geometry deformation is a charge and spin cloud which is also localized in the center of the chain with half widths comparable to that of the geometry deformation. In the case of the parameter set Ib, the half width of the polaron (4δ) is smaller than for the parameter set Ia (7δ). The polaron represents itself by a small equidistant segement in the center of the deformation. The half width is converged with increasing chain length around a value of $N = 50$. The results of the optimizations are given in Fig. 6 for the case $N = 70$ and parameter set Ib.

The energy eigenvalues indicate that two levels in the gap are associated with the polaron which are shifted from the lower and the upper band edge, respectively, into the gap. However, in contrast to SSH results[1] the two levels are not symmetric to midgap. We do not want to discuss the actual energy values for these levels, because, as it is well known, HF levels cannot be directly connected to the measured spectra, but additional correlation corrections, exciton shifts, and probably a different parametrization would be necessary for this purpose.

Next we examine the case of the doubly-charged chain. Figure 7 shows geometry optimizations for parameter set Ia using AUHF and UHF for comparison. In the case of UHF and $N = 56$ [see Figs. 7(a)–7(c)], a bipolaron structure is formed, which changes to two (overlapping) polarons for $N = 116$ [Figs. 7(d)–7(f)]. So in the case of UHF, the formation of a bipolaron for $N = 56$ is clearly a confinement effect of the small chain, a result which is consistent with the findings of Shimoi and Abe.[31] The problem is the large spin contamination of the UHF solution: The calculated value of $5.89\hbar^2$ for $N = 116$ is too large to give the result physical significance. Thus we performed the same calculations also with the AUHF method. We found that projecting out the spin contaminations leads to a RHF solution, which is not necessarily so in the case of a closed-shell AUHF calculation, resulting in a bipolaron structure (A-B-A) having a (quite broad) half width of about 33δ, but with a total energy about 0.7 eV above the UHF solution. Making the same series of calculations for parameter set Ib, we found a similar behavior: In this case, already for $N = 56$ a pair of polarons is formed in the UHF calculation (with even larger spin contamination) and for $N = 116$, the structure of the two separated polarons is more pronounced than in case Ia, the AUHF result again gives a bipolaron. We conclude from these results (the behavior of which can be reproduced with any of the parameter sets investigated here), that despite the higher total energy of the AUHF solution and as we are clearly outside of the dissociation region (where AUHF does not work, see Sec. II A above), the AUHF result is physically

TABLE II. Sets Ia,b and IIa–c of parameters used in our simulations.

Set	Ia	Ib	IIa	IIb	IIc
a_1 (eV/Å)	0.067 957	0.061 379	0.059 587	0.065 876	0.069 416
a_2 (eV/Å)	0.070 439	0.062 760	0.054 751	0.065 268	0.068 728
b_1 (eV)	3.1	1.9	2.0	2.8	3.6
b_2 (eV)	3.045 105	1.865 050	1.981 153	2.764 389	3.565 256
E^D (meV/CH), $N = 69$	27.386	37.533	14.155	5.380	2.090
E^{DD} (meV/CH), $N = 69$	0.188	1.742	8.138	2.472	1.015

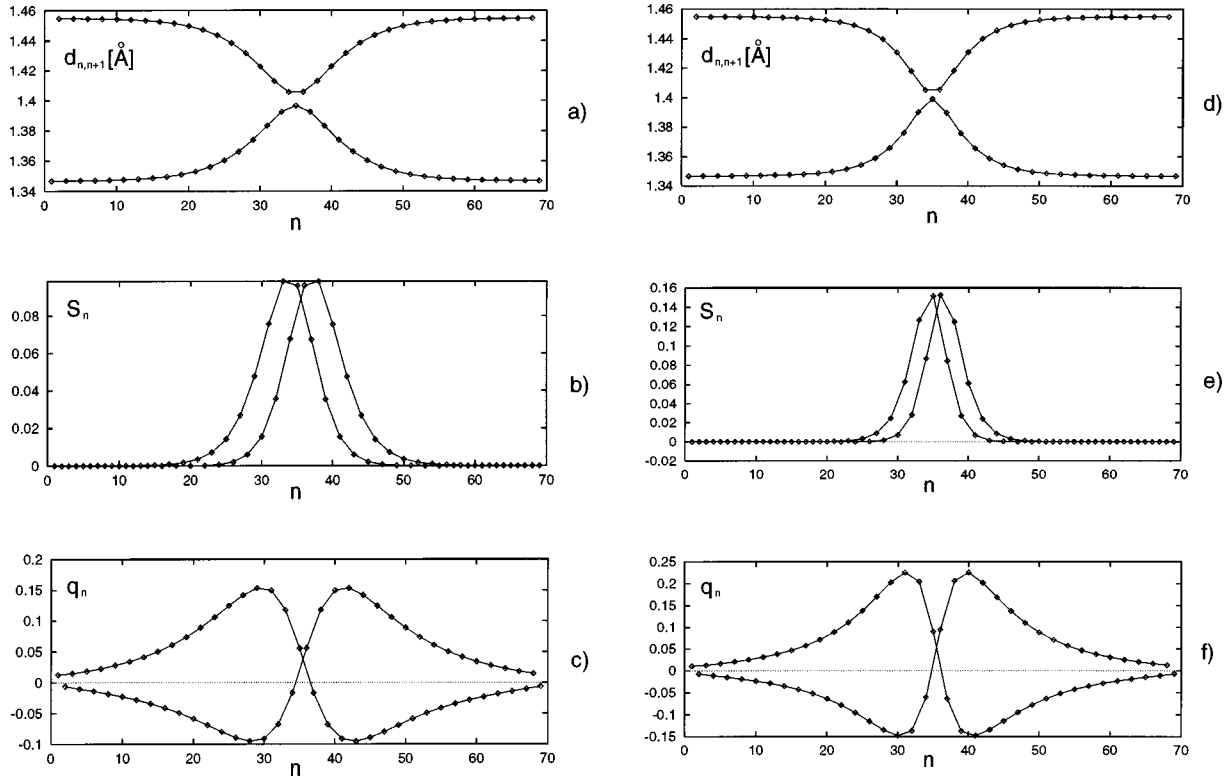

FIG. 6. The bond distances (a,d) $d_{n,n+1}$ between sites n and $n+1$ where the upper line connects even to odd and the lower one odd to even numbered sites, respectively, the spin densities $S_n=(P^{\alpha}_{nn}-P^{\beta}_{nn})$ (b,e) and the charge densities $q_n=1-(P^{\alpha}_{nn}+P^{\beta}_{nn})$ (c,f) where the two lines connect the densities between odd and between even numbered sites n, respectively, in the two plots. (a), (b), and (c) are for parameter set Ia, (d), (e), and (f) for parameter set Ib, both for $N=70$ and a singly-charged chain.

more meaningful because of the quite large spin contamination in the UHF calculation.

The remaining question is that of the width of the *B* phase with increasing chain length, because up to now it is not clear if the *A*-*B*-*A* structure is really a bipolaron or, as in *t*PA, a soliton-antisoliton pair, where the distance increases linearly with the chain length. In our case, the electron-electron interaction is not treated as a free parameter in the model, and thus—based on the results of SSH-like models[1,12,27]—it makes sense to assume that varying the symmetry-breaking E^{DD} should change the bipolaron width, a smaller bipolaron for larger E^{DD} and vice versa. To investigate this, we made a series of AUHF calculations with parameter sets IIa–c (which offers a larger variation in E^{DD} than sets Ia, b), varying the chain length from $N=56$ to $N=200$. The resulting converged bipolaron widths (see Fig. 8) show the expected behavior of the system: for small E^{DD}, the width is converging quite slowly, while for larger values (here 8 meV), a smaller bipolaron width of about 25δ can be observed. Figure 9 shows converged geometries and charge densities (the spin densities are nearly zero) of the resulting structures for $N=200$. For the parameter sets Ia and Ib we find a convergence comparable to that of IIc, which is to be expected from the small value of E^{DD}. We conclude that for doubly charged chains in the ground state, a bipolaron is formed within the range of parameters investigated. The actual width of the bipolaron for realistic parameters is hard to determine because of the quite large variations of E^{DD} in the *ab initio* results quoted above.

IV. DYNAMICS

In the dynamic simulations we use $\Delta t=0.05$ fs, while some simulations performed with $\Delta t=0.001$ fs show the same results. Also simulations with analytical (approximate) and numerical gradients, respectively, show comparable results. First we followed the time evolution of a singly-charged chain with $N=70$, starting with the ground-state geometry for the parameter set Ia. The results are shown in Fig. 10.

Obviously, in the first femtoseconds a polaron is formed as one expects from the optimizations. However, due to the excess energy the ideal polaron structure is somewhat overshot and then the system bounces back close to the starting structure, while the excess energy excites lattice vibrations. After this first oscillation we observe further ones, however, with a more complicated structure due to the excess energy. The spin and charge densities, as well as the lattice deformation, remain localized around the center of the chain, however, the spin density at some times suddenly vanishes, which raises the question, whether the AUHF iterations at these times do not converge to unphysical solutions. This is supported by the fact that the error in energy conservation becomes larger than the kinetic energy which is shown in Fig. 14(a). At the present stage of our investigations we are forced to leave this question open. The parameter set Ib yields similar results.

In Fig. 11 we show the results of a corresponding simulation for a doubly-charged chain with $N=100$ for parameter set Ia. Here we find again the formation of a bipolaron at

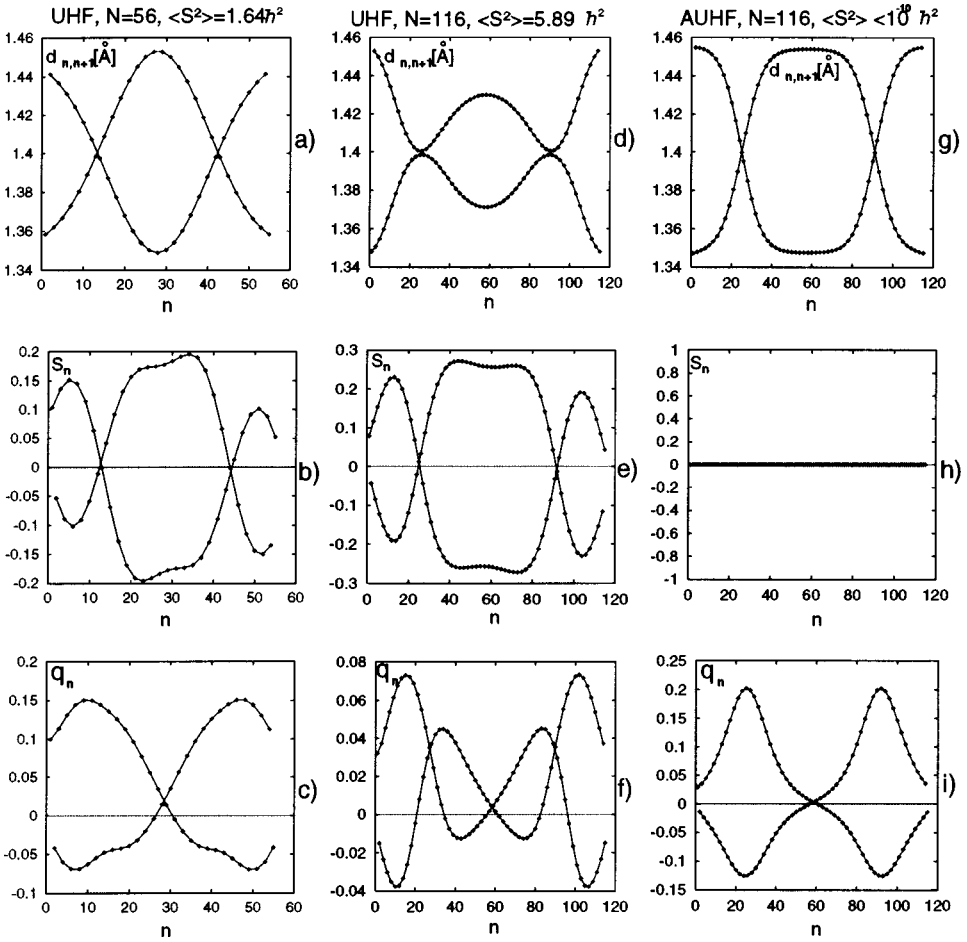

FIG. 7. Comparison of UHF and AUHF, doubly-charged chain. First column: $N=56$, UHF; second column: $N=116$, UHF; third column: $N=116$, AUHF. First row: bond distances $d_{n,n+1}$; second row: spin density S_n; third row: charge density q_n. The lines connect even- and odd-numbered sites, respectively. Parameter set Ia.

times where deep minima of the total potential energy are observed. When bouncing back the initial geometry is overshot and at the maxima of the potential energy we find structures of the type *A-B-A-B-A* corresponding to the formation of two tightly bound polarons. However, the bipolaron is definitely the stable structure, favored by 17.5 meV/CH over the two polarons [Fig. 14(b)]. The geometry and the charge density perform sinusoidal oscillations around the bipolaron structure, where the frequency of the charge-density oscillation is half that of the geometry oscillation. This is similar to the findings in a SSH model, however, there the frequency is one-fourth as Wang, Su, and Martino reported.[29] The results for parameter set Ib are similar and thus not shown here.

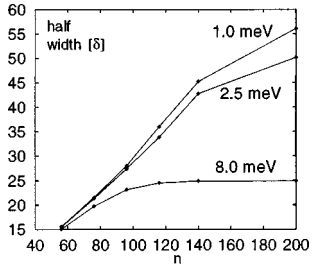

FIG. 8. Converged bipolaron widths for $N=56$, 76, 96, 116. Parameter sets IIa,b,c.

Finally, we want to discuss the mobility of polarons. For this purpose we place the optimum geometry of the charged polaron close to the chain end of a chain of 70 units and follow the dynamics evolving from this initial geometry in the singly charged chain. The results for parameter set I are shown in Fig. 12.

Obviously, the polaron structure accompanied by its spin and charge cloud moves without any change of its form through the chain and is reflected at the chain end. The excess energy, as Fig. 12(a) indicates, is radiated into lattice phonons. It is interesting to observe that the kinetic energy of the chain is nearly constant from 20 to 100 fs [Fig. 14(c)] and does not change as the polaron is reflected at the chain end. For larger simulation times, the kinetic energy increases exponentially, the whole chain starts to vibrate and the moving structure—lattice deformation plus spin and charge cloud—is destroyed. But still, charge as well as spin density stay localized even at larger simulation times. Of course, also the error in energy conservation increases dramatically after 120 fs, so a smaller time step or a different integration method would be necessary to follow the dynamics further. The corresponding results for parameter set Ib are shown in Fig. 13.

Due to the larger dimerization energy, the polaron is slower in this case than in the former one. Also the excess

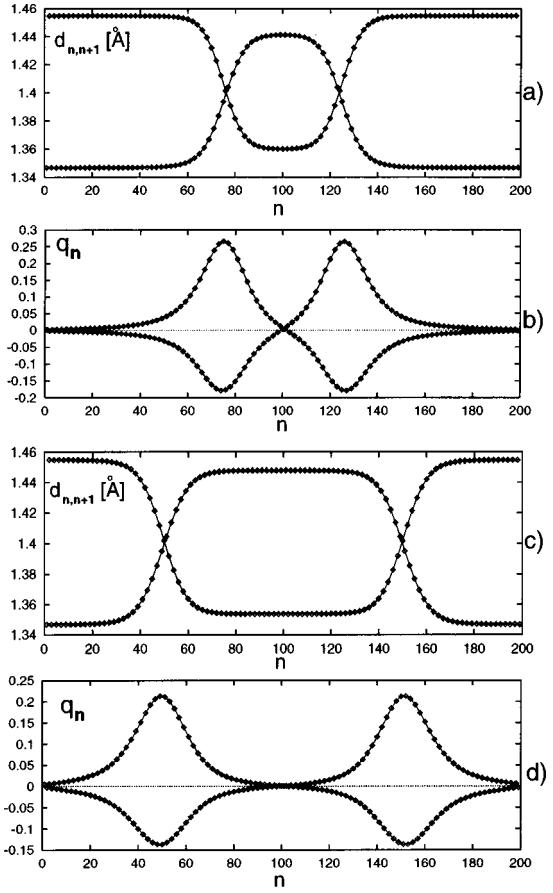

FIG. 9. The bond distances (a,c) $d_{n,n+1}$ between sites n and $n+1$ where the upper lines connect even- to odd- and the lower ones odd- to even-numbered sites and the charge densities $q_n = 1 - (P^{\alpha}_{nn} + P^{\beta}_{nn})$ (b,d) where the lines connect the densities between odd- and even-numbered sites n, respectively, in the two plots. (a) and (b) are for parameter set IIa, (c) and (d) for parameter set IIc, both for $N = 200$ and a doubly-charged chain.

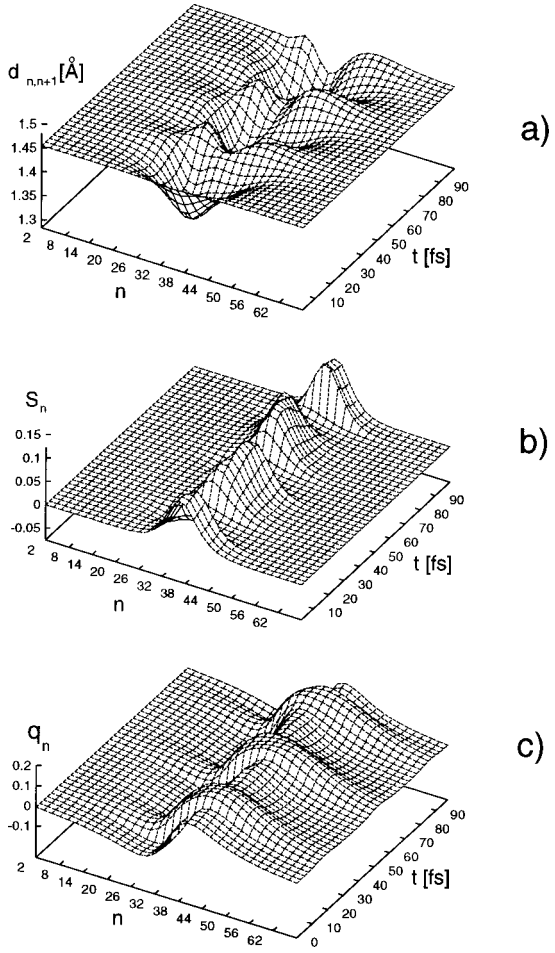

FIG. 10. The time evolution of the bond lengths $d_{n,n+1}(t)$ (for n even) (a), the spin density $S_n(t)$ again for even n only (b) and the charge densities $q_n(t)$ at even sites only (c) for a chain of 70 units and parameter set Ia, starting from the singly charged chain in its equilibrium geometry.

energy is larger and induces large amplitude lattice vibration in another region of the chain than that where the polaron is located. Again around this point in time the errors become too large [Fig. 14(d)] and thus we did not follow the system further.

V. CONCLUSIONS

Our calculations yield several interesting results: One is the stability of the bipolaron in *c*PA in the AUHF/PPP model, which is a matter of discussion in the literature. The geometry optimization, as well as the simulations starting from a doubly-charged chain in equilibrium geometry, unambiguously show that. Wang, Su, and Martino[29] got similar results in the simple SSH case. However, a direct comparison between their and our results is not possible since there parametrization leads to a very large symmetry-breaking energy [100 meV/CH for E^{DD} (Ref. 29)]. Shimoi and Abe[16] conclude on the basis of a UHF/PPP model that at low doping levels polarons are favored over bipolarons. The shortcomings of their approach were already discussed above. On the contrary, Wen and Su[34] use an extended Hubbard model and conclude that bipolarons are stable even at large electron-electron interaction. However, the widths of the quasiparticles they obtained differ from ours. On the other hand, the results obtained by Ye *et al.*[13] with the local-density approximation are in fair agreement with ours. The other interesting result is the finding of mobile polarons. The simulations with a singly-charged polaron on the chain end illustrate the quasiparticle character of the polaron, which is weakened at larger simulation times by lattice phonons. Our results also show the possibility of polarons and bipolarons acting as charge carriers.

For obtaining these results, we have developed a methodology for the parametrization of the PPP Hamiltonian for *c*PA which can be applied in a similar fashion to other conducting polymers. We emphasize here that reparametrizations are indispensible if semiempirical Hamiltonians are used for the description of polymers with different geometrical structures.

ACKNOWLEDGMENTS

The financial support of the ''Deutsche Forschungsgemeinschaft'' (Project No. Fo 175/3-1) and the ''Fond der Chemischen Industrie'' is gratefully acknowledged.

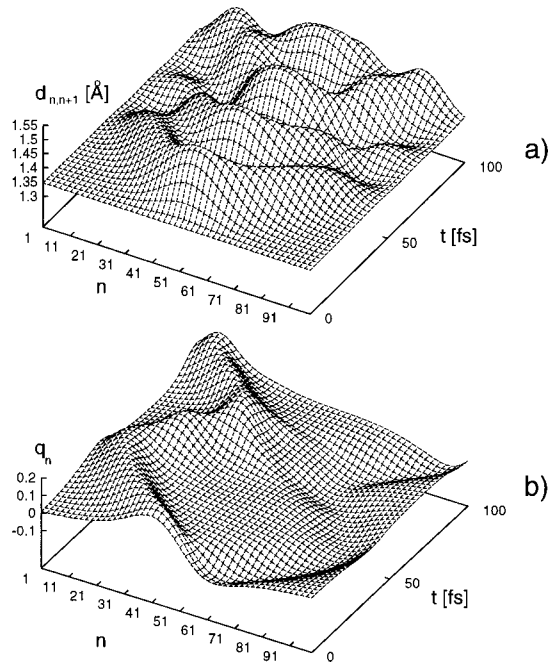

FIG. 11. The time evolution of the bond lengths $d_{n,n+1}(t)$ (for n odd only) (a) and the charge densities $q_n(t)$ at odd sites only (b) for a chain of 100 units and parameter set Ib, starting from the doubly-charged chain in its equilibrium geometry.

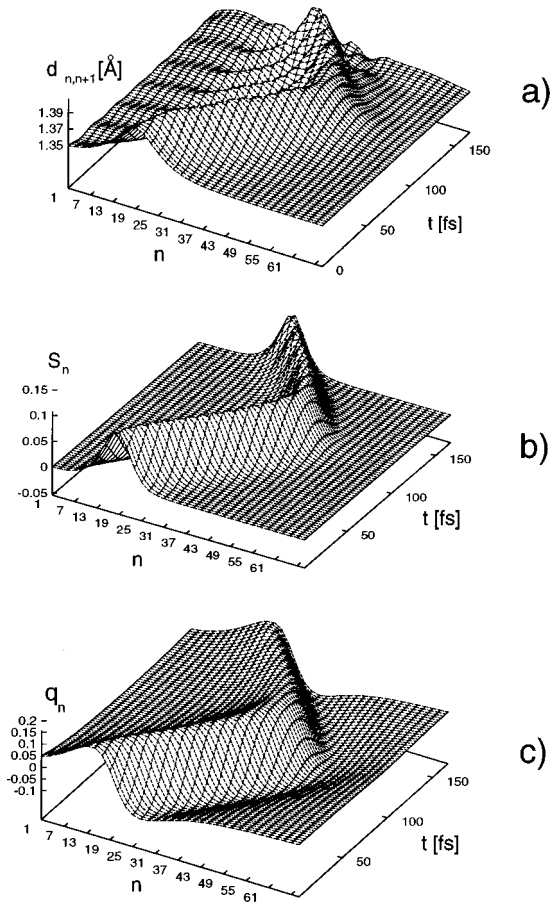

FIG. 12. The time evolution of the bond lengths $d_{n,n+1}(t)$ (for n odd) (a), the spin density $S_n(t)$ again at odd n only (b), and the charge densities $q_n(t)$ at odd sites only (c) for a chain of 70 units and parameter set Ia, starting from the singly-charged chain with the optimized polaron distortion placed close to chain end.

APPENDIX A: THE GEOMETRY OF *c*PA

Our aim is to describe a chain of N CH units in *cis* conformation, with the help of one degree of freedom per CH group, such that it describes the transition from the A to the B phase. First of all we had to determine the geometrical parameters of the stable A phase. For this purpose we performed a full geometry optimization on a small segment of a *c*PA chain, namely *cis*-hexatriene with the help of the *ab initio* HF method corrected for electron correlation with the many-body perturbation theory of second order in Møller-Plesset partitioning (MP2) using the program package GAUSSIAN94.[52] For our optimization we used a valence split basis set augmented by d-type polarization functions on carbon and p-type ones on hydrogen [6-31G** (Ref. 52)]. The results of this optimization are given in Fig. 15.

Of the numbers given in Fig. 15 we use the bond lengths d_1^{tc} and d_2^{tc} together with the bond angle γ_{tc} (index tc denotes trans-cisoid, index ct cis-transoid) of the central unit to construct the geometry of a *c*PA chain in the A phase. In Fig. 16 we show details of the resulting geometry used for the definition of the coordinates $u(i)$ for the CH units. To obtain the geometry of the B phase and the coordinate $u(i)$ we define the following operations: (1) Exchange of the bond lengths, (2) the crossing points of the chain axis with the bond d_2^{tc} are conserved, and (3) each CH group is free to move on a straight line (g) defined by its position in the A and in the B phase, respectively.

Then the position vector of the CH group i is given by $\underline{r}_d(i)$, which is based on the *ab initio* calculations on hexatriene, and $u(i)$, the generalized displacement coordinate:

$$\underline{g}(i)=\frac{1}{2}\,(\underline{r}_{ct}(i)-\underline{r}_{tc}(i)),$$

$$\underline{r}(i)=\underline{r}_d(i)+u(i)\underline{g}(i). \tag{A1}$$

Thus for undistorted chains the generalized coordinate is ($u_0=1$ Å)

$$u(i)=\begin{cases} u_0 & \text{cis-transoid} \\ 0 & \text{equidistant} \\ -u_0 & \text{trans-cisoid.} \end{cases} \tag{A2}$$

The quantities defined in Fig. 16 are calculated as

$$\alpha_{tc}=\pi-\gamma_{tc}; \quad x_{tc}=\frac{1}{2}\,d_2^{tc}\cos(\alpha_{tc}); \quad h_{tc}=\frac{1}{2}\,d_2^{tc}\sin(\alpha_{tc}),$$

$$x_g=x_{tc}+\frac{1}{2}\,d_1^{tc}; \quad x_{ct}=x_g-\frac{1}{2}\,d_2^{tc}; \quad \alpha_{ct}=a\cos\left(\frac{2x_{ct}}{d_1^{tc}}\right), \tag{A3}$$

and

$$h_{tc}=\frac{1}{2}\,d_1^{tc}\sin(\alpha_{ct}); \quad \underline{g}=\frac{1}{2}\begin{pmatrix} x_{tc}-x_{ct} \\ h_{tc}-h_{ct} \end{pmatrix}. \tag{A4}$$

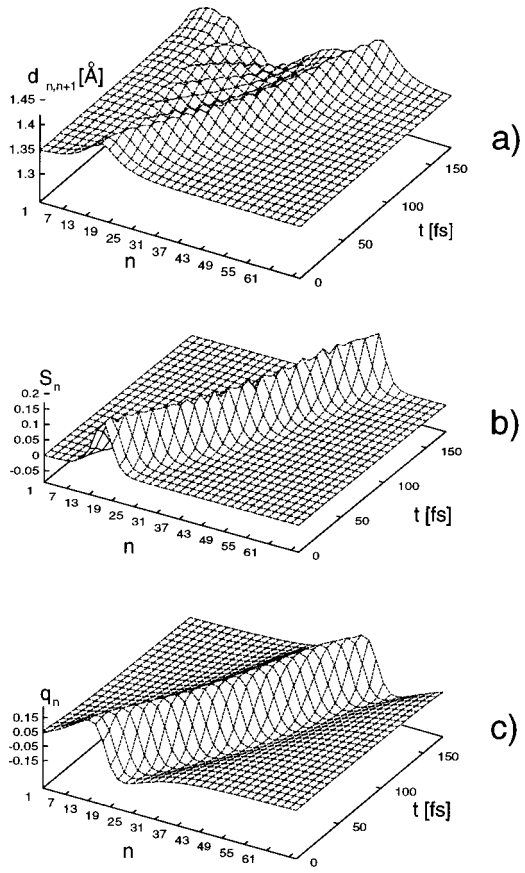

FIG. 13. The time evolution of the bond lengths $d_{n,n+1}(t)$ (for n odd) (a), the spin density $S_n(t)$ again at odd n only (b), and the charge densities $q_n(t)$ at odd sites only (c) for a chain of 70 units and parameter set Ib, starting from the singly-charged chain with the optimized polaron distortion placed close to chain end.

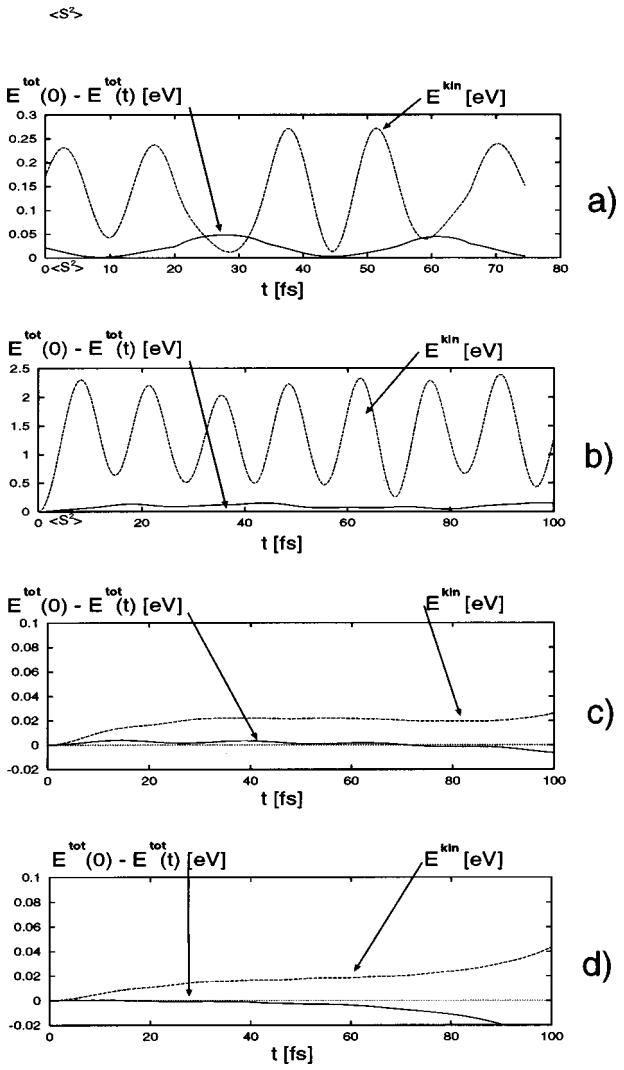

FIG. 14. Kinetic energy and error in energy conservation for the time simulations: (a) singly-charged chain, starting from equilibrium, parameter set Ia (see Fig. 10), (b) doubly-charged chain, starting from equilibrium, parameter set Ia (see Fig. 11), (c) singly-charged chain, starting with polaron at the chain end, parameter set Ia (see Fig. 12), (d) as before, parameter set Ib (see Fig. 13).

With the numbers from Fig. 15, g is then numerically

$$g=\begin{pmatrix}0.025\,874\,987\,2\\0.013\,745\,635\,7\end{pmatrix}. \tag{A5}$$

Assuming that a *c*PA chain always starts with a bond parallel and below the chain axis on its left-hand side, we can write the position vectors of all its units i as

$$\underline{r}(i)=\underline{r}_d(i)+u(i)\underline{\underline{A}}(\mathrm{mod}_4(i-1))\underline{g}=\underline{r}_d(i)+u(i)\underline{g}(i), \tag{A6}$$

where

$$\underline{\underline{A}}(0)=\begin{pmatrix}-1&0\\0&-1\end{pmatrix};\quad \underline{\underline{A}}(1)=\begin{pmatrix}1&0\\0&-1\end{pmatrix},$$

$$\underline{\underline{A}}(2)=\begin{pmatrix}1&0\\0&1\end{pmatrix};\quad \underline{\underline{A}}(3)=\begin{pmatrix}-1&0\\0&1\end{pmatrix}. \tag{A7}$$

The distance between two CH units i and j is given by

$$R_{ij}=\sqrt{[\underline{r}(i)-\underline{r}(j)]^2}$$
$$=\sqrt{[\underline{r}_d(i)-\underline{r}_d(j)+u(i)\underline{g}(i)-u(j)\underline{g}(j)]^2}, \tag{A8}$$

and its derivative is calculated as

$$\frac{\partial R_{ij}}{\partial u(k)}=\frac{1}{R_{ij}}[\underline{r}(i)-\underline{r}(j)][\underline{g}(i)\,\delta_{ik}-\underline{g}(j)\,\delta_{jk}]. \tag{A9}$$

Note, that this definition of the generalized displacement coordinates does not lead to a bond angle γ of 120° for the equidistant chain $[u(i)=0]$, but to an angle of 124°, which is a nevertheless reasonable value for that quantity.

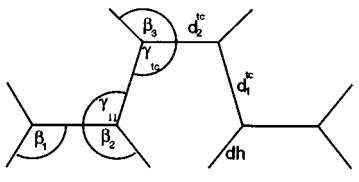

β_1	117.6425°
dh	1.0828Å
d_1^{tc}	1.3493Å
β_2	118.4932°
γ_{tc}	125.1470°
d_2^{tc}	1.4528Å
β_3	121.3040°
γ_{11}	121.4882°

FIG. 15. Optimized geometry of *cis*-hexatriene (HF/MP2 with 6-31G** basis).

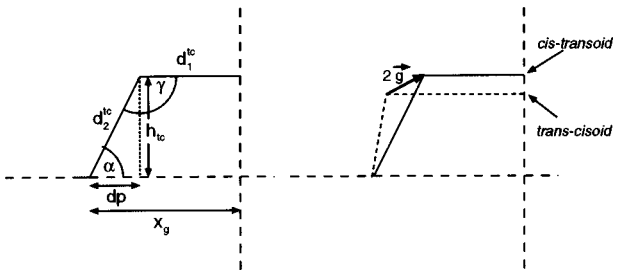

FIG. 16. Details of the geometry of *c*PA used for the definition of the coordinate $u(i)$.

APPENDIX B: σ-ELECTRON ENERGY

The σ bond can be assumed as being well localized, and thus the total σ-electron energy can be written as a sum of pair potentials between next neighbors. We use a Taylor expansion of the energy of a σ bond between unit i and j in the bond length $R_{i,i+1}$ truncated after the harmonic term:

$$E^{\sigma}=E_0^{\sigma}+A\sum_{i=1}^{N-1}(R_{i,i+1}-R_0)+\frac{K}{2}\sum_{i=1}^{N-1}(R_{i,i+1}-R_0)^2$$
$$=E_0^{\sigma}+E_{i,i+1}^{\sigma}, \tag{B1}$$

where R_0 denotes the equilibrium length of a free CC single bond and we use the value $R_0=1.54$ Å (see, e.g., Ref. 53).

Since we need only relative energies and energy derivatives for our study, we can set $E_0^{\sigma}=0$. For the determination of the other two parameters we impose two conditions on the σ potential. First of all the potential has to have its minimum at $R_{i,i+1}=R_0$ by definition for all i. This leads to the condition

$$\frac{dE_{i,i+1}^{\sigma}}{dR_{i,i+1}}=0\Rightarrow A=0. \tag{B2}$$

The remaining parameter K follows from the condition that the total energy of a chain has to be minimal in the ideally dimerized geometry of the A phase $[u(i)=u_0$ in our case]:

$$\sum_{i=1}^{N-1}\left(\left.\frac{\partial E^{\pi}}{\partial u(i)}\right|_{u(i)=u_0}+\left.\frac{\partial E^{nn}}{\partial u(i)}\right|_{u(i)=u_0}+\left.\frac{\partial E^{\sigma}}{\partial u(i)}\right|_{u(i)=u_0}\right)=0. \tag{B3}$$

This condition yields for K the expression

$$K=-\frac{\sum_{i=1}^{N}([\partial E^{\pi}/\partial u(i)]|_{u(i)=u_0}+[\partial E^{nn}/\partial u(i)]|_{u(i)=u_0})}{\sum_{i=1}^{N-1}\sum_{j=1}^{N}(R_{i,i+1}-R_0)[\partial R_{i,i+1}/\partial u(j)]|_{u(j)=u_0}}. \tag{B4}$$

This expression allows us to compute uniquely the value of K for a given set of parameters and a given length of the chain, ensuring thus that the A phase is an energy minimum. Note, that in contrast to *t*PA the minimum of the potential is not exactly at $u(i)=0$ for odd-numbered chains, but we have

$$\left.\frac{dE^{\sigma}}{du}\right|_{u=0}\neq 0. \tag{B5}$$

The deviation of the position of the maximum of E^{σ} from the equidistant chain is only 0.002 32 Å.

APPENDIX C: GRADIENTS OF THE π ENERGY

Förner[54,55] had derived an analytical expression for the calculation of the gradient of the π-electron energy in the case of the UHF method from the converged density matrices ($\underline{\underline{P}}^{\sigma}$). Using the variational theorem on which the UHF method is based one can show that

$$\frac{\partial E_{\mathrm{UHF}}}{\partial u(j)}=\frac{\partial E_{\mathrm{UHF}}^{\pi}+\partial E_{\mathrm{UHF}}^{nn}}{\partial u(j)}$$
$$=\frac{1}{2}\sum_{t=1}^{N}(1-\delta_{jt})\frac{\partial\gamma_{jt}}{\partial u(j)}\{P_{jj}(P_{tt}-2z_t)$$
$$+P_{tt}(P_{jj}-2z_j)+2z_tz_j-2[(P_{jt}^{\alpha})^2+(P_{jt}^{\beta})^2]\}$$
$$+2\sum_{t=1}^{N}\frac{\partial\beta_{jt}}{\partial u(j)}P_{jt};$$

$$P_{jt}\equiv P_{jt}^{\alpha}+P_{jt}^{\beta} \tag{C1}$$

holds, where the z_j are the charges of the ionic cores at unit j (here the ions are all CH^+ ions and thus $z_j=1$). The derivatives of the γ_{jt} and the β_{jt} can be trivially calculated analytically.

Unfortunately, this simple expression holds strictly only for the UHF case, while in AUHF there would occur in addition a very complicated term which contains derivatives of the density-matrix elements. Therefore, one can use alternatively the numerical derivative

$$\frac{\partial E_{\mathrm{AUHF}}[u(1),\ldots,u(N)]}{\partial u(j)}\approx\frac{1}{2h}\{E_j^{\mathrm{AUHF}}(-h)-E_j^{\mathrm{AUHF}}(+h)\},$$

$$E_j^{\mathrm{AUHF}}(\pm h)=E^{\mathrm{AUHF}}[u(1),\ldots,u(j)\pm h,\ldots,u(N)]. \tag{C2}$$

The necessary magnitude of h can be estimated analytically (see Ref. 46). In Ref. 46 also other methods for the calculation of numerical derivatives are described, for example an extrapolation for h approaching zero. However, for the application of such methods the determination of the AUHF energy for at least 10–12 values of h is necessary, and thus they would be too costly computationally, especially for larger chains. The optimum value for h can be also estimated from comparisons between numerical and analytical gradients of the UHF method where Eq. (C1) is exact.

We investigated numerically if Eq. (C1) could be used as an approximation to the true gradient also in the AUHF model. It turned out that in the case of geometry optimizations and time simulations, the error made by application of Eq. (C1) to AUHF is negligibly small. The error in the geometries obtained, in fact, is beyond the convergence criterion. However, Eq. (C1) cannot be used in cases where the zeroes of derivatives have to be computed as exactly as possible, which is necessary for the parametrization. Since in this case we only need to treat short chains, the application of Eq. (C2) does not lead to computational problems.

*Author to whom correspondence should be addressed: King Fahd University of Petroleum and Minerals, Chemistry Department, Dhahran 31261, Saudi Arabia.

[1] A. J. Heeger, S. Kivelson, J. R. Schrieffer, and W.-P. Su, Rev. Mod. Phys. **60**, 781 (1988).
[2] R. E. Peierls, *Quantum Theory of Solids* (Clarendon, Oxford, 1955).
[3] W.-P. Su, J. R. Schrieffer, and A. J. Heeger, Phys. Rev. Lett. **42**, 1698 (1979).
[4] W.-P. Su, J. R. Schrieffer, and A. J. Heeger, Phys. Rev. B **22**, 2988 (1980).
[5] M. Takayama, Y. R. Lin-Liu, and K. Maki, Phys. Rev. B **21**, 2388 (1980).
[6] H. Thomann, L. R. Dalton, Y. Tomkiewicz, N. S. Shiren, and T. C. Clarke, Phys. Rev. Lett. **50**, 533 (1983).
[7] H. Thomann, H. Kim, A. Morrobel-Sosa, L. R. Dalton, M. T. Jones, B. H. Robinson, T. Clarke, and Y. Tomkiewicz, Synth. Met. **9**, 255 (1984).
[8] H. Thomann, J. E. Cline, B. M. Hofmann, H. Kim, A. Morrobel-Sosa, B. H. Robinson, and L. R. Dalton, J. Phys. Chem. **89**, 1994 (1985).
[9] A. J. Heeger and J. R. Schrieffer, Solid State Commun. **48**, 207 (1983).
[10] Z. G. Soos and S. Ramashesha, Phys. Rev. Lett. **50**, 1938 (1983).
[11] M. Sasai, Synth. Met. **9**, 295 (1984).
[12] C.-L. Wang and F. Martino, Phys. Rev. B **34**, 5540 (1986).
[13] L. Ye, A. J. Freeman, D. E. Ellis, and B. Delley, Phys. Rev. B **40**, 6285 (1989).
[14] W. Förner, C. Wang, F. Martino, and J. Ladik, Phys. Rev. B **37**, 4567 (1988).
[15] W. Förner, Adv. Quantum Chem. **25**, 207 (1994).
[16] Y. Shimoi and S. Abe, Synth. Met. **69**, 687 (1995).
[17] L. Rodriguez-Monge and S. Larsson, J. Chem. Phys. **102**, 7106 (1995).
[18] G. Rossi and W. F. Schneider, J. Chem. Phys. **104**, 9511 (1996).
[19] W. Förner, Chem. Phys. **160**, 173 (1992).
[20] T. Amos and L. C. Snyder, J. Chem. Phys. **41**, 1973 (1773).
[21] W. Förner, Chem. Phys. **160**, 189 (1992).
[22] J. L. Bredas, J.-M. Andre, and J. Delhalle, J. Mol. Struct. **87**, 237 (1982).
[23] T. Ito, H. Shirakawa, and S. Ikeda, J. Polym. Sci., Polym. Lett. Ed. **13**, 1943 (1975).
[24] S. Suhai, J. Chem. Phys. **73**, 3843 (1980).
[25] L. W. Schacklette, R. R. Chance, D. M. Ivory, G. G. Miller, and R. H. Baughman, Synth. Met. **1**, 307 (1979).
[26] K. K. Kanazawa, A. F. Diaz, R. H. Geiss, W. D. Gill, J. F. Kwak, J. A. Logan, J. F. Rabolt, and G. B. Street, J. Chem. Soc. Chem. Commun. **1979**, 347.
[27] S. A. Brazovskii and N. Kirova, JETP Lett. **33**, 4 (1981).
[28] A. J. Heeger, Comments Solid State Phys. **10**, 53 (1981).
[29] C.-L. Wang, Z. P. Su, and F. Martino, Phys. Rev. B **33**, 1512 (1986).
[30] Y. Shimoi and S. Abe, Phys. Rev. B **49**, 14 113 (1994).
[31] A. Shimoi and S. Abe, Phys. Rev. B **50**, 14 781 (1994).
[32] M. Springborg, Phys. Rev. B **33**, 8475 (1986); Synth. Met. **28**, D527 (1989).
[33] J. L. Bredas, R. R. Chance, and R. Silbey, Phys. Rev. B **26**, 5843 (1982).
[34] G. Wen and W.-P. Su, Synth. Met. **78**, 195 (1995).
[35] R. Pariser and P. G. Parr, J. Chem. Phys. **21**, 660 (1953).
[36] R. Pariser and P. G. Parr, J. Chem. Phys. **21**, 707 (1953).
[37] J. A. Pople, Trans. Faraday Soc. **49**, 1375 (1953).
[38] J. Ladik, D. K. Rai, and K. Appel, J. Mol. Spectrosc. **27**, 72 (1968).
[39] J. Ladik, Acta Phys. Acad. Sci. Hung. **18**, 186 (1965).
[40] J. Ladik, *Quantenchemie* (Enke, Stuttgart, 1973).
[41] K. Ohno, Theor. Chim. Acta **2**, 219 (1964).
[42] W. Förner, Phys. Rev. B **44**, 11 743 (1991).
[43] F. Martino and J. Ladik, J. Chem. Phys. **52**, 2262 (1970).
[44] I. Mayer, J. Ladik, and B. Biczo, Int. J. Quantum Chem. **7**, 583 (1973).
[45] T. Kovar, Master's thesis, University Erlangen-Nürnberg, Germany, 1987.
[46] W. H. Press, S. A. Teukolsky, W. T. Vetterling, and B. P. Flannery, *Numerical Recipes in FORTRAN* (Cambridge University Press, Cambridge, 1995).
[47] S. Suhai, Phys. Rev. B **51**, 16 553 (1995).
[48] A. Karpfen and R. Höller, Solid State Commun. **37**, 179 (1981).
[49] R. Dovesi, Int. J. Quantum Chem. **26**, 197 (1984).
[50] C. R. Fincher Jr., C. E. Chen, A. J. Heeger, A. G. MacDiarmid, and J. B. Hastings, Phys. Rev. Lett. **48**, 100 (1982).
[51] H. Kahlert, O. Leitner, and G. Leising, Synth. Met. **17**, 467 (1987).
[52] M. J. Frisch, G. W. Trucks, H. B. Schelegel, P. M. W. Gill, B. G. Johnson, M. A. Robb, J. R. Cheeseman, T. A. Keith, G. A. Petersson, J. A. Montgomery, K. Raghavachari, M. A. Al-Laham, V. G. Zakrzewski, J. V. Ortiz, J. B. Forseman, F. Cioslowski, B. B. Stefanov, A. Nanayakkara, M. Challacombe, C. Y. Peng, P. Y. Ayala, W. Chen, M. W. Wong, J. L. Andres, E. S. Replogle, R. Gomperts R. L. Martin, D. J. Fox, J. S. Binkley, D. J. Defreese, J. P. Baker, J. Steward, M. Head-Gordon, C. Gonzalez, and J. A. Pople, GAUSSIAN94 Revision A.1, 1995.
[53] W. Förner, Synth. Met. **30**, 135 (1989).
[54] W. Förner, Solid State Commun. **63**, 941 (1987).
[55] W. Förner, Indian J. Chem. Sec. A (to be published).